Journal of Materials Chemistry A

PAPER

View Article Online
View Journal | View Issue

Cite this: J. Mater. Chem. A, 2018, 6, 22819

Iodocuprate-containing ionic liquids as promoters for green propulsion†

Kangcai Wang,[ac] Ajay Kumar Chinnam,[a] Natan Petrutik,[a] Eswaravara Prasadarao Komarala,[b] Qinghua Zhang,*[c] Qi-Long Yan,*[d] Roman Dobrovetsky*[a] and Michael Gozin*[a]

Received 18th August 2018
Accepted 17th October 2018

DOI: 10.1039/c8ta08042a

rsc.li/materials-a

In this work, we prepared and comprehensively characterized four novel iodocuprate-containing ionic liquids, CuILs **1–4**. In addition to their interesting molecular structures and physical properties CuILs exhibited capability to efficiently promote hypergolic reactions between boron-containing [EMIM$^+$][H_3BCN^-] and [MIM]·[BH_3] fuels and a highly concentrated H_2O_2 (95%) oxidizer. The most promising promoter CuIL **3** has the decomposition temperature well above the decomposition temperature of the fuels, was stable in promoter-in-fuel mixtures for weeks and showed ignition delay times down to 14 ms. We believe that further development of our new iodocuprate ionic liquids can lead to promising "green" H_2O_2-based bipropellant systems for space applications.

Introduction

Development of new metal-containing ionic liquids (MILs) is an emerging field in chemistry and materials science, as the properties and performance of these compounds have the advantages of both ionic liquids and metal-containing salts and complexes. MILs have a broad range of promising applications, spanning catalysis,[1] materials for biomedicine,[2] optoelectronics,[3] gas fixation,[4] energy storage[5] and conversion,[6] and are quickly expanding to new fields.[7] A sub-group of MILs, containing halogenated metal anions and halogen-metal charged clusters (XMILs), has its own fascinating properties, chemistry and molecular structures.[8] In particular, recently, XMILs containing iodocuprate cluster anions gained a significant attention, due to their interesting supramolecular structures and promising unique photoluminescence properties, suitable for the development of efficient photocatalysts[9] and materials for energy conversion.[10] Despite the frequent use of copper iodide in catalytic carbon–carbon coupling reactions,[11] Buchwald's *N*-arylation,[12] oxidative C–H functionalization of cycloalkanes,[13] conversion of alkynes to alcohols and many other catalytic reactions,[14] iodocuprates are much less explored in terms of the range of their chemical reactivity.[15] To the best of our knowledge, there are no reports regarding the use of iodocuprates as oxidation or combustion catalysts.

Due to our general interest in the development of novel promoters for efficient hypergolic ignition of energetic ionic liquid fuels with an environmentally safe non-cryogenic highly concentrated H_2O_2 (>90%; HTP) oxidizer for space propulsion, we designed, prepared, comprehensively characterized, and evaluated the properties and performance of a series of new iodocuprate-containing ionic liquids (CuILs), as novel combustion catalysts. These CuILs include salts of 3-ethyl-1-methyl-1*H*-imidazol-3-ium [EMIM$^+$]$_4$[$Cu_4I_8^{4-}$] (CuIL **1**), [EMIM$^+$]$_3$[$Cu_4I_7^{3-}$] (CuIL **2**), and [EMIM$^+$]$_2$[$Cu_5I_7^{2-}$] (CuIL **3**), and a salt of 1-amino-3-methyl-1*H*-imidazol-3-ium [MATA$^+$][CuI_2^-] (CuIL **4**).

Notably, many energetic ionic liquids (EILs) were evaluated as "green" bipropellant fuels,[16] having low vapor pressure, as high density thermostable alternatives to toxic hydrazines.[17] It was found that EILs would exhibit hypergolic ignition when in contact with fuming nitric acid or dinitrogen tetroxide oxidizers. Yet, the toxicity and corrosivity of these oxidizers, as well as the formation of nitrogen oxide (NO_x) gases during the combustion process, have still been a challenging problem that requires a solution. A "green" hypergolic oxidizer for the EIL fuels could be HTP, as an alternative to fuming nitric acid and dinitrogen tetroxide.[18] Until recently, only few attempts were made to use HTP as a "green" hypergolic oxidant,[19,20] where Natan and coworkers found that hypergolic ignition of gelated hydrocarbon fuel could be achieved with HTP through the addition of catalytic particles.[21] Rarata and co-workers reported metal halogen based promoted hypergolic ignitions of

[a]School of Chemistry, Faculty of Exact Science, Tel Aviv University, Tel Aviv, 69978, Israel. E-mail: rdobrove@post.tau.ac.il; cogozin@gmail.com

[b]Department of Materials Science and Engineering, Tel Aviv University, Tel Aviv, 69978, Israel

[c]Research Center of Energetic Materials Genome Science, Institute of Chemical Materials (ICM), China Academy of Engineering Physics (CAEP), Mianyang, 621900, China. E-mail: qinghuazhang@caep.cn

[d]Science and Technology on Combustion, Thermo-structure, and Internal Flow Laboratory, Northwestern Polytechnical University, Xian, 710072, China. E-mail: qilongyan@nwpu.edu.cn

† Electronic supplementary information (ESI) available. CCDC 1855164–1855167. For ESI and crystallographic data in CIF or other electronic format see DOI: 10.1039/c8ta08042a

kerosene, methanol, ethanol, isopropanol, ethylene glycol and ethyl acetate, with HTP,[22] while hypergolic ignition of quaternary trihexyltetradecylphosphonium aluminum borohydride [THTDP$^+$][Al(BH$_4$)$_4^-$] EIL with HTP was reported by Schneider.[23] Choi and coworkers also investigated hypergolic ignitions of a series of heterocyclic organic salts with HTP, using promoters.[24] Hypergolic reactions of HTP with boron-free EILs, such as 1-butyl-3-methylimidazolium azide [BMIM$^+$][N$_3^-$], 2-hydroxyethylhydrazinium nitrate [HEH$^+$][NO$_3^-$], dimethylammoniumethyleneazido trifluoroacetate [DMAZ$^+$][TFA$^-$] and dimethylammoniumethyleneazido dicyanamide [DMAZ$^+$][DCA$^-$], promoted by 1-butyl-3-methyl-imidazolium [BMIM$^+$][FeCl$_4^-$] catalyst, were also reported.[25]

Our novel CuILs were designed to provide effective solutions to a series of significant issues. Since a quick hypergolic ignition of EILs with H_2O_2 could not be typically achieved without use of promoters, these promoters should possess a range of additional essential properties, including forming and keeping stable solutions with EIL fuels, exhibiting thermostability above the decomposition temperature of the EILs (without affecting the inherent thermostability of the fuels) and not affecting the viscosity properties of the fuels.

Results and discussion

Synthesis

Iodocuprate-containing ionic liquid (CuIL) promoters **1–4**, including two multinuclear clusters tetra-(1-ethyl-3-methylimidazolium) tetracopperoctaiodide ([EMIM$^+$]$_4$[Cu$_4$I$_8^{4-}$] – CuIL **1**) and hexa(1-ethyl-3-methylimidazolium) octacoppertetradecaiodide ([EMIM$^+$]$_6$[Cu$_8$I$_{14}^{6-}$] – CuIL **2**) and two coordination polymers poly[bis(1-ethyl-3-methylimidazolium) pentacopperheptaiodide] ([EMIM$^+$]$_{2n}$[Cu$_5$I$_7^{2-}$]$_n$ – CuIL **3**) and poly[1-methyl-4-amino-1,2,4-triazolium copper diiodide] ([MATA$^+$]$_n$[CuI$_2^-$]$_n$ – CuIL **4**) were synthesized in excellent yields (>92%) by solvothermal methodology (Fig. 1). A general procedure included dispersion of CuI powder in a solution of [EMIM$^+$][I$^-$] (or [MATA$^+$][I$^-$]) in methanol and heating the reaction mixture at 90 °C in a sealed glass reactor. After cooling to room temperature, two layers were formed. The bottom layer, containing the desired CuIL product, was separated and washed with methanol. During the washing process the material in the bottom layer crystallized to yield a pure CuIL product.

For CuILs **1–3**, variation of molar ratio between the CuI and [EMIM$^+$][I$^-$] starting materials allowed control over the formation of the specific CuIL product. In contrast, for CuIL **4**, we found that the variation of ratio between CuI and [MATA$^+$][I$^-$] (of 1 : 1, 1 : 3 and 3 : 2, respectively) didn't affect the reaction outcome and the same product (CuIL **4**) was obtained under all explored reaction conditions. These findings demonstrate the unprecedented effect of the counter cation control over the formation and the structure of the specific iodocuprate cluster or coordination polymer product. The phase purities of CuILs **1–4** were confirmed by NMR analysis and powder XRD analysis (Fig. S1–S9, ESI†), and no paramagnetic species were detected in solid-state EPR measurements for all CuILs.

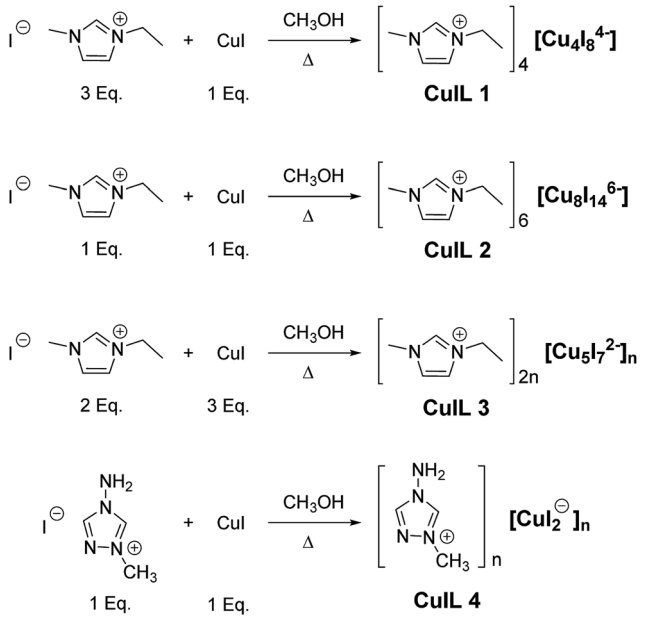

Fig. 1 Synthesis of CuILs **1–4**.

X-ray crystallography

The structures of the promoters CuILs **1–4** were analyzed by single crystal X-ray crystallography. Colorless crystals of CuIL **1** (CCDC 1855164†), with a crystal density of 2.491 g cm^{-3} at 173 K, were obtained by crystallization of CuIL **1** from methanol solution and have the triclinic space group $P\bar{1}$ (Table S1, ESI†). There are two different copper atoms, four iodine atoms and two [EMIM$^+$] cations in the asymmetric unit of CuIL **1** (Fig. 2a). Metal center Cu1 is trigonally coordinated to three iodine atoms, to form a planar trigonal CuI$_3$ group, while metal center Cu2 is tetrahedrally coordinated to four iodine atoms, to form a tetrahedron CuI$_4$ group (Fig. 2b). The Cu–I bond lengths are in the range of 2.517(1)–2.919(1) Å (ESI†). The adjacent CuI$_3$ and CuI$_4$ groups are connected to each other through the edge-sharing mode to form a [Cu$_4$I$_8^{4-}$] cluster, where the face of the CuI$_3$ group is oriented towards the tetrahedral face of CuI$_4$, with the Cu1···I1 distance of 2.919(1) Å (Fig. 2c). The negative charge of the [Cu$_4$I$_8^{4-}$] cluster is balanced by four [EMIM$^+$] cations, while the cluster is interacting with surrounding cations through I···H–C hydrogen bonds, with the I···C distances in the range of 3.103(2)–3.158(3) Å (Fig. 2d).

Colorless crystals of CuIL **2** (CCDC 1855165†), with a crystal density of 2.673 g cm^{-3} at 173 K, were obtained by crystallization of CuIL **2** from methanol solution and have the triclinic space group $P\bar{1}$ (Table S1, ESI†). In the asymmetric unit of CuIL **2** there are four different copper atoms (Cu1, Cu2, Cu3, and Cu4), seven iodine atoms and three [EMIM$^+$] cations (Fig. 3a). In CuIL **2**, each copper metal center is coordinated to four iodine atoms to form a tetrahedral structure, where the Cu–I bond length is in the range of 2.517(2) Å–2.919 (2) Å (Fig. 3b). The adjacent CuI$_4$ tetrahedra in the cluster of **2** are connected to each other by edge- and face-sharing modes, to form a [Cu$_8$I$_{14}^{6-}$] multinuclear anion with a linear arrangement (Fig. 3c). Alternatively, the unprecedented structure of the

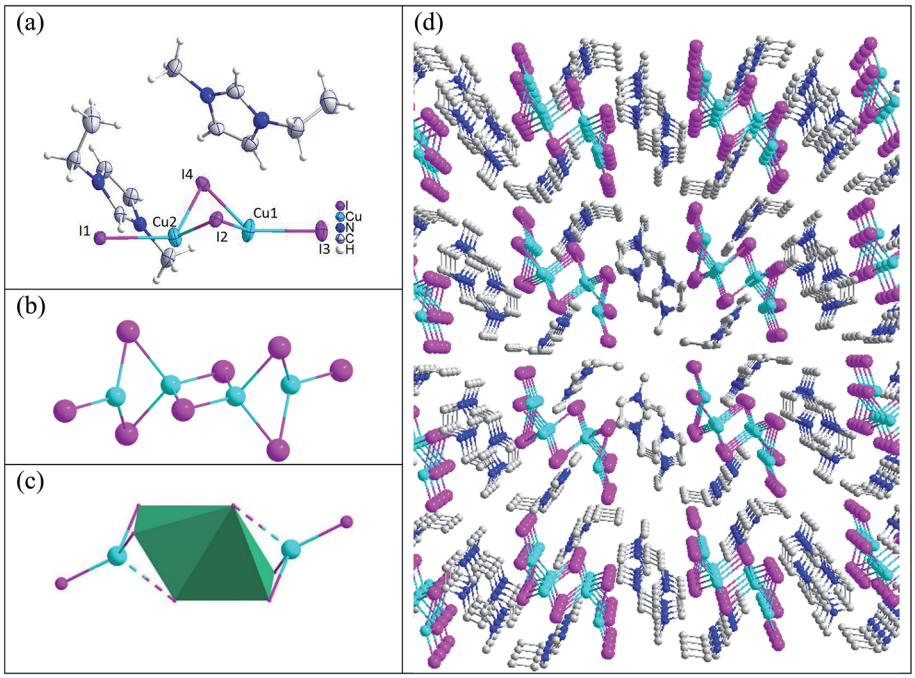

Fig. 2 Structure of CuIL **1**. (a) Molecular structure of CuIL **1**; (b) structure of the $[Cu_4I_8^{4-}]$ cluster inside CuIL **1**; (c) additional presentation mode of the $[Cu_4I_8^{4-}]$ cluster structure; and (d) crystal structure of CuIL **1**.

$[Cu_8I_{14}^{6-}]$ cluster can be described as a connection of four edge-linked $[Cu_2I_5^{3-}]$ trigonal bipyramids, each of which is formed by two face-sharing copper iodine tetrahedra.

Colorless crystals of CuIL **3** (CCDC 1855166†), with a crystal density of 3.235 g cm^{-3} at 173 K, were obtained by crystallization of CuIL **3** from methanol solution and have the orthorhombic space group *Pnma* (Table S1, ESI†). There are two and a half different copper atoms, two and three halves of iodine atoms and one $[EMIM^+]$ cation in the asymmetric unit of CuIL **3** (Fig. 4a). The structure of the coordination polymeric anion containing the $[Cu_5I_7^{2-}]$ repeating unit is based on adjacent CuI_3 and CuI_4 moieties, where three of the CuI_4 tetrahedra are interacting with each other through edge-sharing (Fig. 4c). The Cu–I bond length in CuIL **3** was found to be in the range of

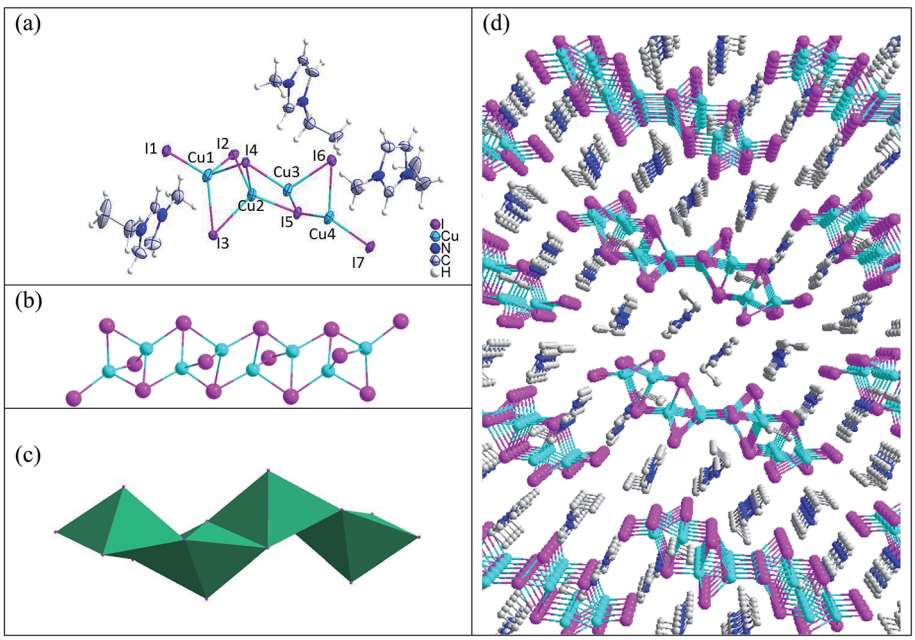

Fig. 3 Structure of CuIL **2**. (a) Molecular structure of CuIL **2**; (b) structure of the $[Cu_8I_{14}^{6-}]$ cluster inside CuIL **2**; (c) additional presentation mode of the $[Cu_8I_{14}^{6-}]$ cluster structure; and (d) crystal structure of CuIL **2**.

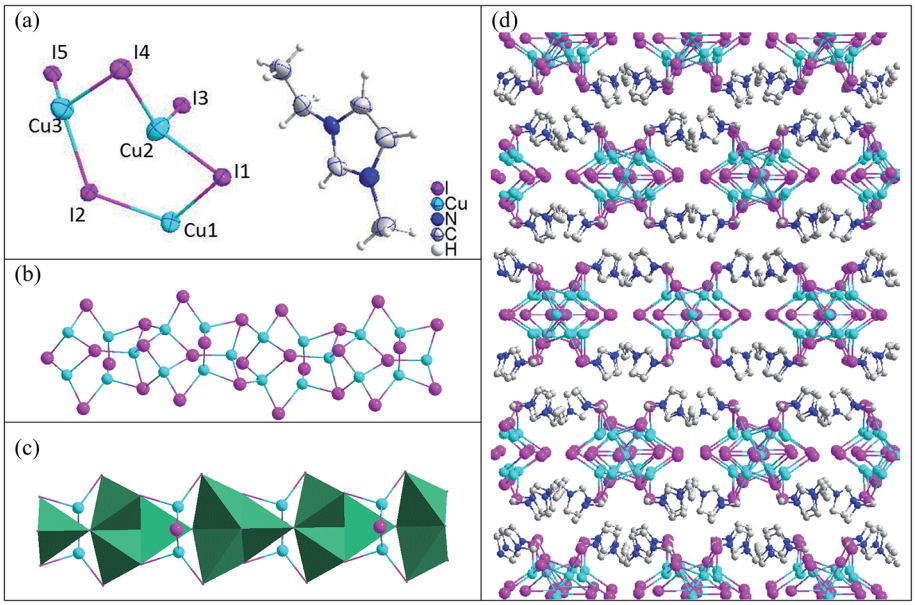

Fig. 4 Structure of CuIL **3**. (a) Molecular structure of CuIL **3**; (b) structure of the $[Cu_5I_7^{2-}]$ cluster inside CuIL **3**; (c) additional presentation mode of the $[Cu_5I_7^{2-}]$ cluster structure; and (d) crystal structure of CuIL **3**.

2.575(2)–2.750(2) Å. The adjacent parallel chains of $[Cu_5I_7^{2-}]_n$ are interacting with each other through $[EMIM^+]$ counter cations *via* I···H–C hydrogen bonds, with the I···C distance being in the range of 3.689(2)–3.940(3) Å (Fig. 4d).

Colorless crystals of CuIL **4** (CCDC 1855167†), with a crystal density of 2.885 g cm^{-3} at 173 K, were obtained by the crystallization of CuIL **4** from methanol solution and have the monoclinic space group $P2_1/n$ (Table S1, ESI†). The asymmetric unit of CuIL **4** contained one copper atom, two iodine atoms and one $[MATA^+]$ cation (Fig. 5a). Each copper atom is coordinated to four adjacent iodine atoms to form a CuI_4 tetrahedron (Fig. 5b). Furthermore, in CuIL **4**, the structure of the coordination polymeric anion containing $[CuI_2^-]$ repeating unit is based on adjacent CuI_4 tetrahedra that are interacting with each other through edge-sharing (Fig. 5c). The Cu–I bond length in CuIL **4** was found to be in the range of 2.648(2)–2.611(2) Å. Notably, along the [001] direction in the crystals of CuIL **4**, linear channels are formed by an arrangement of $[MATA^+]$ counter cations, where these channels are filled with chains of $[CuI_2^-]_n$ coordination polymers (Fig. 5d).

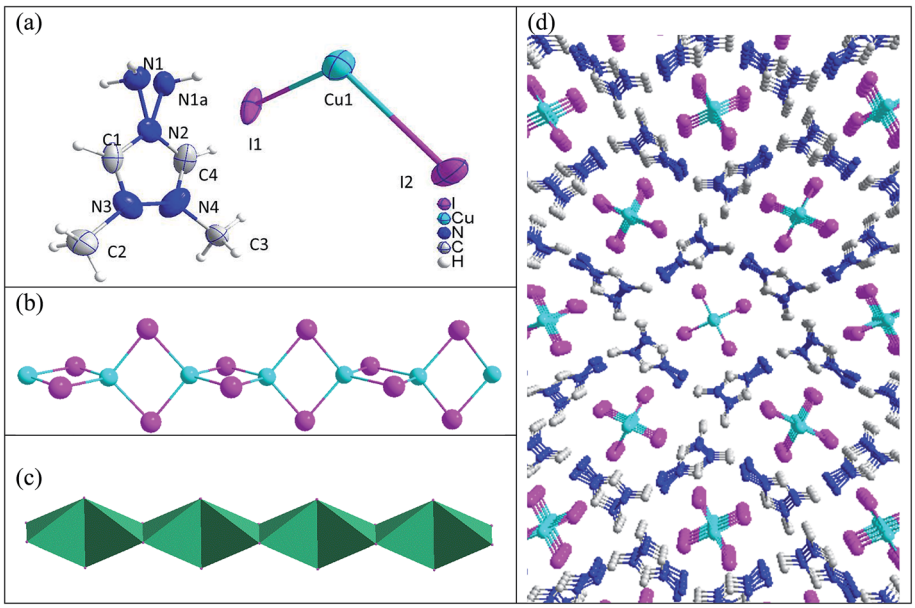

Fig. 5 Structure of CuIL **4**. (a) Molecular structure of CuIL **4**; (b) structure of the $[CuI_2^-]_n$ cluster inside CuIL **4**; (c) additional presentation mode of the $[CuI_2^-]_n$ cluster structure; and (d) crystal structure of CuIL **4**.

The phase purities of CuILs **1–4** were confirmed by powder XRD analysis (Fig. S9, ESI†). Morphologies of the CuIL **1–4** crystals were examined and the corresponding SEM images of these crystals are shown in Fig. S10 (ESI†).

Thermal analysis

The thermal properties of CuILs **1–4** were measured by differential scanning calorimetry (DSC) and thermo-gravimetric analysis (TGA). The DSC curves that were obtained for CuILs **1–4** showed endothermic peaks corresponding to the melting processes at 69, 73, 80 and 84 °C (Fig. S15, ESI†), which was surprisingly low considering these compounds' molecular structures. The TGA results confirmed that the observed endotherms belong to the melting process and not to the decomposition process, as no weight loss was observed below 100 °C for any of these compounds (Fig. 6). The decomposition temperatures of CuILs **1–3** were found to be at 295, 298 and 303 °C, with the weight loss of 56.3, 43.9 and 39.8% from room temperature to 500 °C, respectively. A somewhat higher thermostability of CuIL **3** could be explained by its more rigid "reinforced concrete"-type molecular structure (*versus* non-polymeric CuILs **1** and **2**), due to the presence of the $[Cu_5I_7^{2-}]_n$ polymeric anion. We believe that a similar chemical composition of CuILs **1–3** is the major reason for the significant degree of similarity in the thermal properties (similar TGA curves) of these compounds. In comparison, CuIL **4** exhibited poor thermostability, with the decomposition temperature of 160 °C and the weight loss of 53.1% from room temperature to 500 °C. Searching the literature, we found that EMIM-based ionic liquids were at least by 100 °C more thermostable than their MATA analogues.[26] For example, $[EMIM^+][I^-]$ and $[EMIM^+][N(CN)_2^-]$ ionic liquids exhibit decomposition temperatures of 249 °C and 275 °C, respectively, while the corresponding $[MATA^+][I^-]$ and $[MATA^+][N(CN)_2^-]$ salts have respective decomposition temperatures of 136 °C and 175 °C.[27] These results are perfectly in line with our observations for the prepared CuILs, in which the decomposition temperature of $[MATA^+]_n[CuI_2^-]_n$ **4** is lower than that of the EMIM-based salts **1–3** by 140 °C, clearly indicating the critical importance of the cation component in the thermostability of these compounds, rather than the structure of the anionic part.

Physical properties of fuels containing CuIL promoters

The density, viscosity, thermostability and heat of combustion, and specific impulse (I_{sp}) are important properties of propellant fuels. In this work, in order to study the effect of adding different CuIL promoters to the ionic and non-ionic "green" liquid hypergolic fuels $[EMIM^+][H_3BCN^-]$ (**F1**)[28] and $[MIM]\cdot[BH_3]$ (**F2**),[29] each of the CuILs **1–4** (10 wt%) were added to each fuel, respectively. As shown in Table 1, the densities of **F1** and **F2** are 0.980 and 0.930 g cm^{-3}, respectively. After the addition of promoters, the densities of the fuels slightly increased. In particular, when mixed with 10 wt% of CuIL **3**, the densities of **F1** and **F2** increased up to 1.025 and 1.010 g cm^{-3}, respectively, which is due to the highest density of promoter **3** (3.235 g cm^{-3}). Although addition of 10 wt% CuILs to the examined **F1** and **F2**

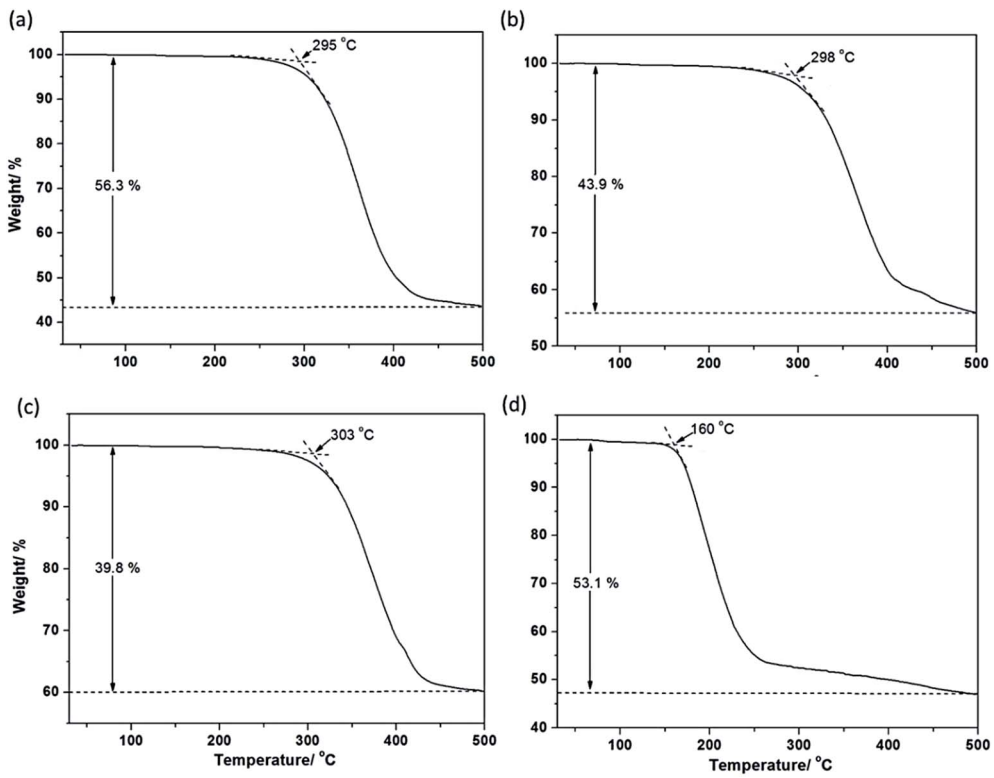

Fig. 6 TG curves: (a) CuIL **1**, (b) CuIL **2**, (c) CuIL **3** and (d) CuIL **4**.

Table 1 Physicochemical properties of the hypergolic fuels with and without CuILs

	Fuel	Promoter	T_d[a] (°C)	ρ[b] (g cm^{-3})	η[c] (mPa s)	ΔH_c[d] (kJ g^{-1})	I_{sp}[e] (s)	ID[f] (ms)
1	**F1**	No	247	0.980	19	−34.06	269.0	>1000
2	**F1**	1	220	1.018	42	−31.48	264.7	37
3	**F1**	2	221	1.021	48	−31.22	261.3	36
4	**F1**	3	219	1.025	50	−31.56	263.9	24
5	**F1**	4	214	1.023	55	−32.55	262.3	38
6	**F2**	No	263	0.930	5	−36.17	266.6	>300
7	**F2**	1	161	1.005	80	−32.96	262.5	30
8	**F2**	2	162	1.007	87	−33.86	259.1	23
9	**F2**	3	160	1.010	82	−33.35	261.7	14
10	**F2**	4	158	1.008	89	−33.76	260.1	28

[a] Decomposition temperature. [b] Density at 25 °C. [c] Viscosity at 25 °C. [d] Calculated heat of combustion, based on bomb calorimetry measurements. [e] I_{sp} values for promoter-in-fuel mixtures that were calculated from the I_{sp} values of the pure fuels **F1** and **F2** and CuIL promoters. [f] Ignition delay times.

fuels also leads to an increase in the viscosity of the resulting mixtures (Table 1), the resulting viscosity in the range of 40–90 mPa s is well below that of other well-explored promoter-free energetic ionic liquids.[30] We found that addition of promoters CuIL **1–4** to the evaluated fuels resulted in decreased decomposition temperatures of the fuel mixtures to about 30–100 °C for **F1** and **F2** (Table 1). Despite a reduction in overall thermostability of promoter–fuel mixtures, the decomposition temperatures of the **F1** mixtures with CuIL **1–4** are still above 214 °C (*versus* 247 °C of the parent fuel), clearly exhibiting suitability of our promoters for further development. We also studied the stability of promoter–fuel mixtures for four weeks by using ^{1}H NMR (Fig. S12–S19, ESI†), finding that during all periods of study, these examined mixtures didn't show any detectable impurities and degradation products. The I_{sp} values of pure fuels and examined promoter-in-fuel mixtures are shown Table 1. In comparison to the pure **F1** and **F2** fuels, the calculated I_{sp} values for the examined promoter-in-fuel mixtures are slightly lower (by 1.6–2.8%), which could be explained by EXPLO5 (v6.02) algorithms that do not take into account possible changes in combustion mechanisms that may take place upon the introduction of promoters with lower I_{sp} (Tables S10 and S11, ESI†).

Hypergolic ignition tests

The performance of CuILs **1–4** as promoters of hypergolic ignition with highly concentrated H_2O_2 (95%) was evaluated for the hypergolic fuels **F1** and **F2**. All ignition experiments were conducted under the ambient conditions, utilizing "oxidizer-to-fuel" droplet addition methodology (Table 1, Fig. 7 and S20–S27, ESI†). In a typical experiment, a single droplet of H_2O_2 (15 μL) was added using micropipette to an Eppendorf plastic tube, containing the fuel **F1** or **F2** (150 μL) and a tested CuIL promoter (10 wt%). All ignition tests were filmed with a high-speed camera, operated at 6000 frames s^{-1}, assessing ignition delay (ID) times with the precision of 0.17 ms. The ID times were measured from the initial contact of the H_2O_2 drop with the promoter–fuel mixture until the appearance of a clearly detectable flame. Reference ignition tests, in which a single drop of H_2O_2 (95%) was added to promoter-free **F1** and **F2** fuels, showed relatively long ID times of more than 1000 ms and 300 ms, respectively (Table 1). For comparison, Shreeve and Zhang reported that hypergolic fuels **F1** and **F2**, in combination with *WFNA* as an oxidant, showed ID times of 4 ms and 6 ms, respectively.[28,31]

In our evaluation of hypergolic ignitions of CuIL **1**-containing fuels **F1** and **F2** (with highly concentrated H_2O_2), we observed 10-fold shortened ID times (*versus* promoter-free ignitions) of 37 ms and 30 ms, respectively. We also found that the promoter CuIL **2** was able to reduce the ID times for **F1** and **F2** fuels to 39 ms and 23 ms, respectively, while the best-performing promoter was found to be CuIL **3**, exhibiting impressive ID times for **F1** and **F2** of 24 ms and 14 ms, respectively (Fig. 7). In a subsequent set of experiments with CuIL **4**, we found ID times of 38 ms and 28 ms, respectively (Table 1). The results obtained for CuILs **1–4** indicate that the structure of the polymeric anion $[Cu_5I_7^{2-}]_n$ in **3** is the most suitable for the efficient iodocuprate-based promotion of the studied hypergolic reactions with H_2O_2.

The concluding step in our studies was concentration-dependent performance experiments with both fuels **F1** and **F2**, in which we measured variations in ID times as a function of CuIL **3** concentration in these fuels (1, 2, 5, 8, 10 and 15 wt%; Fig. 7c). We found that for both fuels **F1** and **F2**, no significant changes in ID times were observed for promoter **3** concentrations above 10 wt%, indicating that this concentration could be the optimum for further development of these bipropellant systems.

Proposed reaction mechanism

As a starting point, we assumed that our reaction works in a similar fashion to the non-radical reaction model proposed previously by Liebhafsky[32–34] and Furrow,[35] which is a two-step reaction of HI with H_2O_2 in a 1 : 2 ratio. Initially, the HI reacts with the first equivalent of H_2O_2, producing HOI and H_2O (eqn (1)). In the second step, HOI reacts with the second equivalent of H_2O_2, producing O_2 and another molecule of H_2O with the regeneration of HI (eqn (2)).

$$HI + H_2O_2 \rightarrow HOI + H_2O \quad (1)$$

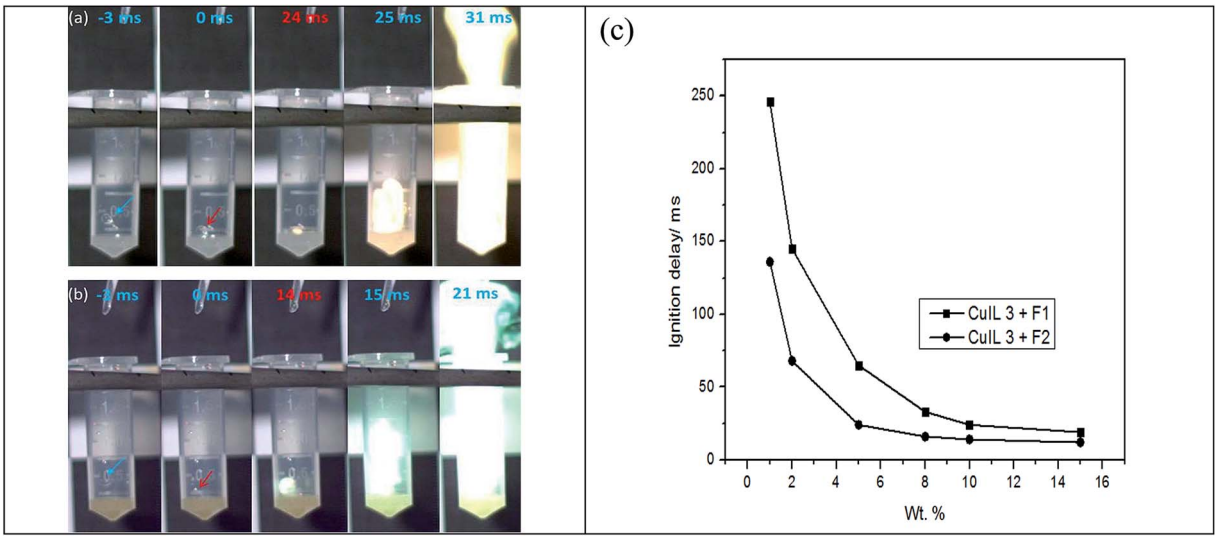

Fig. 7 Fast camera images from the hypergolic ignition tests with H_2O_2 (95%) and CuIL **3** as a promoter. (a) Using **F1** as a fuel; (b) using **F2** as a fuel; and (c) results of hypergolic ignition tests with H_2O_2 (95%), **F1** and **F2** fuels and CuIL **3** as a promoter.

$$HOI + H_2O_2 \rightarrow O_2 + H_2O + HI \quad (2)$$

In contrast to the reaction described above, in our case it is likely that CuILs **1–4** react with H_2O_2 instead of HI. To check whether this mechanistic perspective makes sense from a thermodynamic point of view, we performed the density functional theory (DFT) calculation at the wB97XD/def2-SVP level of theory,[36,37] using Stuttgart–Dresden ECP[38] for the relativistic effect of iodine and copper, on the reaction of H_2O_2 with $[CuI_3^{-2}]\cdot 2[EMIM^+]$. Noteworthily, $[CuI_3^{-2}]\cdot 2[EMIM^+]$ was chosen as the mono-nuclear model of the CuIL **1–4** clusters to avoid complications in calculations. Thus based on these calculations, the first step is the pre-coordination of H_2O_2 with $[CuI_3^{-2}]\cdot 2[EMIM^+]$ giving **Int1**, which is formed as a result of a hydrogen bonding between iodine atoms and protons of H_2O_2; this step is exergonic with ΔG of -7.6 kcal mol^{-1}. The next step is the substitution of iodide at the Cu center by H_2O_2 leading to **Int2**; this step is slightly endergonic, $\Delta G = 8.1$ kcal mol^{-1}. The calculated activation barrier for the formation of **Int2** (**TS**) is 8.8 kcal mol^{-1}, which is relatively low. The next two steps closely follow the Liebhafsky and Furrow mechanism. The first of these two steps is the reaction of I^- with the H_2O_2 coordinated to the Cu center in **Int2** forming $[I_2CuOI^{-2}]\cdot 2[EMIM^+]$ (**Int3**) and water, which is strongly exergonic with ΔG of -14.0 kcal mol^{-1}. The second of the steps, which is the reaction of **Int3** with the second equivalent of H_2O_2, giving H_2O, O_2 and regenerated $[CuI_3^{-2}]\cdot 2[EMIM^+]$, is also exergonic ($\Delta G = -6.5$ kcal mol^{-1}). Overall, this process is strongly exergonic with the release of 20 kcal mol^{-1} Gibbs free energy (Fig. 8).

Experimental

General information

Caution! Proper safety precautions should be taken during the preparation, characterization and handling of energetic ionic liquids and high concentration H_2O_2. Lab personnel and the equipment should be properly grounded, and protective equipment, including protective coat, Kevlar gloves, ear protection and face shield, should be used. All the reactions and hypergolic ignition testing of the prepared materials were conducted in a protected fume hood and behind a safety shield.

$[EMIM^+]_4[Cu_4I_8^{4-}]$ (1). A powder of CuI (0.95 g, 5 mmol) was dispersed in a solution of $[EMIM^+][I^-]$ (3.57 g, 15 mmol) in methanol (10 mL) and the reaction mixture was heated at 90 °C for 30 min in a sealed glass reactor. After cooling the reaction mixture to room temperature, two layers were formed and the bottom layer, containing the desired product, was separated and washed with cold methanol (3 × 3 mL). During the washing process, the liquid product solidified into a white powder of pure compound **1** (2.10 g, 98% yield; based on Cu). Mp (DSC

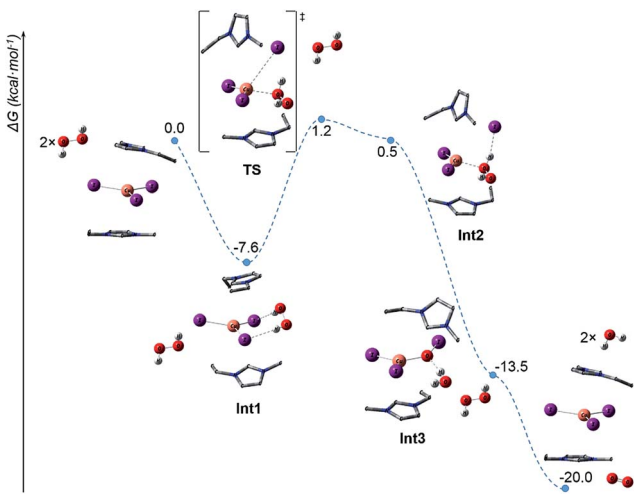

Fig. 8 Proposed calculated mechanisms of plausible H_2O_2 decomposition in the presence of the CuIL model promoter $[EMIM^+]_2[CuI_3^{2-}]$. Gibbs free energies are given relatively to the starting materials.

peak, 10 °C min^{-1}, N_2): 69 °C. ^{1}H NMR (400 MHz, DMSO-d_6) δ: 9.10 (s, 1H), 7.76 (s, 1H), 7.68 (s, 1H), 4.16–4.22 (q, 2H), 3.84 (s, 3H), 1.41 (t, 3H). ^{13}C NMR (100 MHz, DMSO-d_6) δ: 136.0, 123.4, 121.9, 44.1, 35.8, 15.1. FTIR (ATR): 3265 (w), 3069 (m), 2979 (w), 1605 (w), 1559 (m), 1449 (m), 1341 (w), 1154 (s), 1087 (w), 827 (m), 748 (s), 613 (m).

$[EMIM^+]_6[Cu_8I_{14}{}^{6-}]$ (2). A powder of CuI (1.90 g, 10 mmol) was dispersed in a solution of $[EMIM^+][I^-]$ (2.38 g, 10 mmol) in methanol (10 mL) and the reaction mixture was heated at 90 °C for 30 min in a sealed glass reactor. After cooling the reaction mixture to room temperature, two layers were formed and the bottom layer, containing the desired product, was separated and washed with cold methanol (3 × 3 mL). During the washing process, the liquid product solidified into a white powder of pure compound **2** (3.39 g, 92% yield; based on Cu). Mp (DSC peak, 10 °C min^{-1}, N_2): 73 °C. ^{1}H NMR (400 MHz, DMSO-d_6) δ: 9.09 (s, 1H), 7.75 (s, 1H), 7.67 (s, 1H), 4.16–4.21 (q, 2H), 3.84 (s, 3H), 1.40 (t, 3H). ^{13}C NMR (100 MHz, DMSO-d_6) δ: 135.9, 123.4, 121.8, 44.0, 35.8, 15.0. FTIR (ATR): 3285 (w), 3091 (m), 2985 (w), 1601 (w), 1557 (m), 1447 (m), 1347 (w), 1152 (s), 1095 (w), 817 (m), 739 (s), 606 (m).

$[EMIM^+]_{2n}[Cu_5I_7{}^{2-}]_n$ (3). A powder of CuI (2.85 g, 15 mmol) was dispersed in a solution of $[EMIM^+][I^-]$ (2.38 g, 10 mmol) in methanol (10 mL) and the reaction mixture was heated at 90 °C for 30 min in a sealed glass reactor. After cooling the reaction mixture to room temperature, two layers were formed and the bottom layer, containing the desired product, was separated and washed with cold methanol (3 × 3 mL). During the washing process, the liquid product solidified into a white powder of pure compound **3** (4.23 g, 99% yield; based on Cu). Mp (DSC peak, 10 °C min^{-1}, N_2): 80 °C. ^{1}H NMR (400 MHz, DMSO-d_6) δ: 9.08 (s, 1H), 7.74 (s, 1H), 7.66 (s, 1H), 4.15–4.21 (q, 2H), 3.84 (s, 3H), 1.40 (t, 3H). ^{13}C NMR (100 MHz, DMSO-d_6) δ: 135.9, 123.3, 121.8, 44.0, 35.7, 15.0. FTIR (ATR): 3136 (w), 3098 (m), 2971 (w), 1598 (w), 1557 (m), 1446 (m),1381 (w), 1153 (s), 1097 (w), 813 (m), 740 (s), 611 (m).

$[MATA^+]_n[CuI_2{}^-]_n$ (4). A powder of CuI (1.90 g, 10 mmol) was dispersed in a solution of $[MATA^+][I^-]$ (2.26 g, 10 mmol) in methanol (10 mL) and the reaction mixture was heated at 90 °C for 30 min in a sealed glass reactor. After cooling the reaction mixture to room temperature, two layers were formed and the bottom layer, containing the desired product, was separated and washed with cold methanol (3 × 3 mL). During the washing process, the liquid product solidified into a white powder of pure compound **4** (4.11 g, 99% yield; based on Cu). Mp (DSC peak, 10 °C min^{-1}, N_2): 84 °C. ^{1}H NMR (400 MHz, DMSO-d_6) δ: 10.05 (s, 1H), 9.13 (s, 1H), 6.92 (s, 2H), 4.01 (s, 3H). ^{13}C NMR (100 MHz, DMSO-d_6) δ: 144.7, 142.6, 38.9. FTIR (ATR): 3285 (w), 3208 (w), 3067 (m), 2924 (w), 2855 (w), 1690 (w), 1618 (m), 1560 (w), 1452 (w), 1358 (w), 1159 (m), 1067 (w), 941 (s), 852 (m), 727 (w), 595 (s).

Conclusions

In this work, four novel iodocuprate-containing ionic liquids CuILs **1–4** were synthesized and comprehensively characterized, and their performance as promoters of hypergolic ignition of boron-containing fuels with H_2O_2 was studied. Our new CuILs were found to exhibit intriguing molecular structures and physical properties. We showed that specific CuIL structures could be obtained in excellent yields (>92%), by controlling the molar ratios of the starting materials and by variating the cation structure. Structures of the $[Cu_8I_{14}{}^{6-}]$ cluster in CuIL **2** and the $[Cu_5I_7{}^{2-}]_n$ coordination polymer in CuIL **3** are unprecedented, while examples of the $[Cu_4I_8{}^{4-}]$ cluster (found in CuIL **1**) and the $[CuI_2{}^-]_n$ coordination polymer (found in CuIL **4**) are very rarely observed in hundreds of reported iodocuprate compounds. Taking into account large molecular structures of the resultant CuILs, these materials showed unusually low melting temperatures of below 85 °C, while CuILs **1–3** exhibited decomposition temperatures close to 300 °C. We can conclude that the thermostability of our new CuILs is mostly determined by the nature of the counter cation and not by the structure of the iodocuprate cluster or the coordination polymer. In terms of CuIL performance as promoters of hypergolic ignition with H_2O_2, we found that at the concentration of 10 wt%, CuIL **3** showed the shortest ignition delay times of 24 and 14 ms for $[EMIM^+][H_3BCN^-]$ (**F1**) and $[MIM]\cdot[BH_3]$ (**F2**) fuels, respectively. Also, at the same concentration, CuIL **3** was able to keep the viscosity of the promoter-in-fuel CuIL **3**–**F1** mixture at 50 mPa s and to remain in the **F1** solution for at least four weeks without any signs of its degradation and the degradation of the fuel, showing excellent chemical stability of this promoter-in-fuel mixture. The promising properties and performance as hypergolic ignition promoters (with H_2O_2) of the newly synthesized CuILs, especially of CuIL **3**, can pave the way for the development of green bipropellant systems based on H_2O_2 for space applications.

Conflicts of interest

There are no conflicts to declare.

Acknowledgements

We are thankful to the XIN Center for Nanoscience and Nanotechnology of the Tel Aviv University for supporting this research.

References

1 (*a*) R. Kore, P. Berton, S. P. Kelley, P. Aduri, S. S. Katti and R. D. Rogers, Group IIIA Halo-metallate Ionic Liquids: Speciation and Applications in Catalysis, *ACS Catal.*, 2017, **7**, 7014–7028; (*b*) K. Li, H. Choudhary and R. D. Rogers, Ionic liquids for sustainable processes: Liquid metal catalysis, *Curr. Opin. Green Sustainable Chem.*, 2018, **11**, 15–21.

2 Z. Zheng, J. Guo, H. Mao, Q. Xu, J. Qin and F. Yan, Metal-Containing Poly(ionic liquid) Membranes for Antibacterial Applications, *ACS Biomater. Sci. Eng.*, 2017, **3**, 922–928.

3 (*a*) B. R. Lee, H. Choi, J. S. Park, H. J. Lee, S. O. Kim, J. Y. Kim and M. H. Song, Surface modification of metal oxide using ionic liquid molecules in hybrid organic–inorganic optoelectronic devices, *J. Mater. Chem.*, 2011, **21**, 2051; (*b*)

E. Margapoti, M. Muccini, A. Sharma, A. Colombo, C. Dragonetti, D. Roberto and A. Valore, Optoelectronic properties of OLEC devices based on phenylquinoline and phenylpyridine ionic iridium complexes, *Dalton Trans.*, 2012, **41**, 9227–9231.

4 (*a*) T. Wang, D. Zheng, J. Zhang, B. Fan, Y. Ma, T. Ren, L. Wang and J. Zhang, Protic Pyrazolium Ionic Liquids: An Efficient Catalyst for Conversion of CO_2 in the Absence of Metal and Solvent, *ACS Sustainable Chem. Eng.*, 2018, **6**, 2574–2582; (*b*) M. Liu, J. Lan, L. Liang, J. Sun and M. Arai, Heterogeneous catalytic conversion of CO_2 and epoxides to cyclic carbonates over multifunctional tri-*s*-triazine terminal-linked ionic liquids, *J. Catal.*, 2017, **347**, 138–147; (*c*) D. Kim, Y. Moon, D. Ji, H. Kim and D. Cho, Metal-Containing Ionic Liquids as Synergistic Catalysts for the Cycloaddition of CO_2: A Density Functional Theory and Response Surface Methodology Corroborated Study, *ACS Sustainable Chem. Eng.*, 2016, **4**, 4591–4600; (*d*) J. Sun, S. I. Fujita and M. Arai, Development in the green synthesis of cyclic carbonate from carbon dioxide using ionic liquids, *J. Organomet. Chem.*, 2005, **690**, 3490–3497.

5 (*a*) G. Hernández, M. Isik, D. Mantione, A. Pendashteh, P. Navalpotro, S. Devaraj, R. Marcilla and D. Mecerreyes, Redox-active poly(ionic liquid)s as active materials for energy storage applications, *J. Mater. Chem. A*, 2017, **5**, 16231–16240; (*b*) M. Forsyth, G. M. A. Girard, A. Basile, M. Hilder, D. R. MacFarlane, F. Chen and P. C. Howlett, Inorganic–Organic Ionic Liquid Electrolytes Enabling High Energy-Density Metal Electrodes for Energy Storage, *Electrochim. Acta*, 2016, **220**, 609–617; (*c*) L. Grande, J. Zamory, S. Koch, J. Kalhoff, E. Paillard and S. Passerini, Homogeneous Lithium Electrodeposition with Pyrrolidinium-Based Ionic Liquid Electrolytes, *ACS Appl. Mater. Interfaces*, 2015, **7**, 5950–5958.

6 (*a*) J. Łuczak, M. Paszkiewicz, A. Krukowska, A. Malankowska and A. Zaleska-Medynska, Ionic liquids for nano- and microstructures preparation. Part 1: properties and multifunctional role, *Adv. Colloid Interface Sci.*, 2016, **230**, 13–28; (*b*) W. R. H. Wright, E. R. Berkeley, L. R. Alden, R. T. Baker and L. G. Sneddon, Transition metal catalysed ammonia-borane dehydrogenation in ionic liquids, *Chem. Commun.*, 2011, **47**, 3177–3179.

7 (*a*) B. A. Rosen and I. Hod, Tunable Molecular-Scale Materials for Catalyzing the Low-Over-potential Electrochemical Conversion of CO_2, *Adv. Mater.*, 2018, 1706238; (*b*) A. Zazybin, K. Rafikova, V. Yu, D. Zolotareva, V. M. Dembitsky and T. Sasaki, Metal-containing ionic liquids: current paradigm and applications, *Russ. Chem. Rev.*, 2017, **86**, 1254–1270; (*c*) K. Goossens, K. Lava, C. W. Bielawski and K. Binnemans, Ionic Liquid Crystals: Versatile Materials, *Chem. Rev.*, 2016, **116**, 4643–4807; (*d*) A. S. Amarasekara, Acidic Ionic Liquids, *Chem. Rev.*, 2016, **116**, 6133–6183.

8 (*a*) K. Pradhan, G. L. Gutsev and P. Jena, Negative ions of transition metal–halogen clusters, *J. Chem. Phys.*, 2010, **133**, 144301; (*b*) X.-L. Lv, K. Wang, B. Wang, J. Su, X. Zou, Y. Xie, J.-R. Li and H.-C. Zhou, A Base-Resistant Metalloporphyrin Metal–Organic Framework for C–H Bond Halogenation, *J. Am. Chem. Soc.*, 2017, **139**, 211–217; (*c*) Y. Wang and S. Pan, Recent development of metal borate halides: Crystal chemistry and application in second-order NLO materials, *Coord. Chem. Rev.*, 2016, **323**, 15–35; (*d*) H. Chen, P.-X. Liu, S.-P. Zhuo, X. Meng, Z.-Y. Zhou and H.-N. Wang, A $[Cu_4I]$ cluster-based metal–organic framework to detect F^- ions, *Inorg. Chem. Commun.*, 2016, **63**, 69–73; (*e*) D. Freudenmann, S. Wolf, M. Wolff and C. Feldmann, Ionic Liquids: New Perspectives for Inorganic Synthesis?, *Angew. Chem., Int. Ed.*, 2011, **50**, 11050–11060.

9 (*a*) J. Liu, F. Wang, L. Y. Liu and J. Zhang, Interpenetrated Three-dimensional Copper-Iodine Cluster with Enantiopure Porphyrin-like Templates, *Inorg. Chem.*, 2016, **55**, 1358–1360; (*b*) G. Fumagalli, P. T. G. Rabet, S. Boyd and M. F. Greaney, Three-Component Azidation of Styrene-Type Double Bonds: Light-Switchable Behavior of a Copper Photoredox Catalyst, *Angew. Chem., Int. Ed.*, 2015, **54**, 11481–11484; (*c*) Y. Zhang, M. Schulz, M. Wachtler, M. Karnahl and B. Dietzek, Heteroleptic diamine-diphosphine Cu(I) complexes as an alternative towards noble-metal based photosensitizers: Design strategies, photophysical properties and perspective applications, *Coord. Chem. Rev.*, 2018, **356**, 127–146; (*d*) C. Chen, R.-H. Li, B.-S. Zhu, K.-H. Wang, J.-S. Yao, Y.-C. Yin, M.-M. Yao, H.-B. Yao and S.-H. Yu, Highly luminescent inks: aggregation-induced emission of Cu–I hybrid clusters, *Angew. Chem., Int. Ed.*, 2018, **57**, 7106–7110.

10 (*a*) W. Lin, C. C. Stoumpos, O. Y. Kontsevoi, Z. Liu, Y. He, S. Das, Y. Xu, K. M. McCall, B. W. Wessels and M. G. Kanatzidis, $Cu_2I_2Se_6$: A Metal–Inorganic Framework Wide-Bandgap Semi-conductor for Photon Detection at Room Temperature, *J. Am. Chem. Soc.*, 2018, **140**, 1894–1899; (*b*) J. Conesa-Egea, K. Hassanein, M. Muñoz, F. Zamora and P. Amo-Ochoa, Fast and efficient direct formation of size-controlled nanostructures of coordination polymers based on copper(I)-iodine bearing functional pyridine terminal ligands, *Dalton Trans.*, 2018, **47**, 5607–5613.

11 (*a*) L. Brandsma, H. D. Verkruijsse and S. F. Vasilevsky, Copper-Catalyzed Carbon–Carbon Bond Formation by 1,1- and 1,3-Substitution Reactions, in *Application of Transition Metal Catalysts in Organic Synthesis*, Springer, Berlin, Heidelberg, 1999, pp. 107–139; (*b*) T. S. Ratani, S. Bachman, G. C. Fu and J. C. Peters, Photoinduced, Copper-Catalyzed Carbon–Carbon Bond Formation with Alkyl Electrophiles: Cyanation of Unactivated Secondary Alkyl Chlorides at Room Temperature, *J. Am. Chem. Soc.*, 2015, **137**, 13902–13907.

12 (*a*) J. C. Antilla, A. Klapars and St. L. Buchwald, The Copper-Catalyzed N-Arylation of Indoles, *J. Am. Chem. Soc.*, 2002, **124**, 11684–11688; (*b*) E. R. Strieter, B. Bhayana and S. L. Buchwald, Mechanistic Studies on the Copper-Catalyzed N-Arylation of Amides, *J. Am. Chem. Soc.*, 2009, **131**, 78–88.

13 (*a*) J. Liu, W. Wei, T. Zhao, X. Liu, J. Wu, W. Yu and J. Chang, Iodine/Copper Iodide-Mediated C–H Functionalization:

Synthesis of Imidazo[1,2-*a*]pyridines and Indoles from N-Aryl Enamines, *J. Org. Chem.*, 2016, **81**, 9326–9336; (*b*) X.-X. Guo, D.-W. Gu, Z. Wu and W. Zhang, Copper-Catalyzed C–H Functionalization Reactions: Efficient Synthesis of Heterocycles, *Chem. Rev.*, 2015, **115**, 1622–1651.

14 (*a*) G.-N. Liu, R.-Y. Zhao, H. Xu, Z.-H. Wang, Q.-S. Liu, M. Z. Shahid, J.-L. Miao, G. Chen and C. Li, The structures, water stabilities and photoluminescence properties of two types of iodo-cuprate(I)-based hybrids, *Dalton Trans.*, 2018, **47**, 2306–2317; (*b*) Y. Qiao, P. Hao and Y. Fu, Symmetrically Related Construction and Optical Properties of Two Non-centrosymmetric 3D Iodides of d^{10} Cation (Cu^+, Ag^+) Based on the N-Benzylpyridinium and Its Supramolecular Interactions, *Inorg. Chem.*, 2015, **54**, 8705–8710.

15 (*a*) S.-L. Li, R. Zhang, J.-J. Hou and X.-M. Zhang, Photoluminescent cuprous iodide polymorphs generated *via in situ* organic reactions, *Inorg. Chem. Commun.*, 2013, **32**, 12–17; (*b*) S. L. Li and X. M. Zhang, Cu_3I_7 Trimer and Cu_4I_8 Tetramer Based Cuprous Iodide Polymorphs for Efficient Photocatalysis and Luminescent Sensing: Unveiling Possible Hierarchical Assembly Mechanism, *Inorg. Chem.*, 2014, **53**, 8376–8383.

16 (*a*) S. Schneider, T. Hawkins, M. Rosander, G. Vaghjiani, S. Chambreau and G. Drake, Ionic Liquids as Hypergolic Fuels, *Energy Fuels*, 2008, **22**, 2871–2872; (*b*) V. K. Bhosale, S. G. Kulkarni and P. S. Kulkarni, Ionic Liquid and Biofuel Blend: A Low-cost and High-Performance Hypergolic Fuel for Propulsion Application, *ChemistrySelect*, 2016, **1**, 1921–1925; (*c*) P. D. McCrary, G. Chatel, S. A. Alaniz, O. A. Cojocaru, P. A. Beasley, L. A. Flores, S. P. Kelley, P. S. Barber and R. D. Rogers, Evaluating Ionic Liquids as Hypergolic Fuels: Exploring Reactivity from Molecular Structure, *Energy Fuels*, 2014, **28**, 3460–3473; (*d*) Q. Zhang and J. M. Shreeve, Energetic Ionic Liquids as Explosives and Propellant Fuels: A New Journey of Ionic Liquid Chemistry, *Chem. Rev.*, 2014, **114**, 10527–10574; (*e*) E. Sebastiao, C. Cook, A. Hu and M. Murugesu, Recent developments in the field of energetic ionic liquids, *J. Mater. Chem. A*, 2014, **2**, 8153–8173; (*f*) J. Li, W. Fan, X. Weng, C. Tang, X. Zhang, Z. Huang and Q. Zhang, Experimental Observation of Hypergolic Ignition of Superbase-Derived Ionic Liquids, *J. Propul. Power*, 2018, **34**, 125–132; (*g*) X. Wenga, C. Tanga, J. Li, Q. Zhangc and Z. Huanga, Coulomb explosion and ultra-fast hypergolic ignition of borohydride-rich ionic liquids with WFNA, *Combust. Flame*, 2018, **194**, 464–471.

17 (*a*) T. M. Klapötke and G. Holl, The greening of explosives and propellants using high-energy nitrogen chemistry, *Green Chem.*, 2001, **3**, G75; (*b*) K. Chingin, R. H. Perry, S. D. Chambreau, G. L. Vaghjiani and R. N. Zare, Generation of Melamine Polymer Condensates upon Hypergolic Ignition of Dicyanamide Ionic Liquids, *Angew. Chem., Int. Ed.*, 2011, **50**, 8634–8637; (*c*) K. Farhat, Y. Batonneau, R. Brahmi and C. Kappenstein, *Applications of Ionic Liquids in Science and Technology*, ed. S. T. Handy, InTech., 2011, ch. 21; (*d*) I. Frank, A. Hammerl, T. M. Klapötke and C. Nonnenberg, Processes during the Hypergolic Ignition between Monomethylhydrazine (MMH) and Dinitrogen Tetroxide (N_2O_4) in Rocket Engines, *Propellants, Explos., Pyrotech.*, 2005, **30**, 44–52; (*e*) S. D. Chambreau, S. Schneider, M. Rosander, T. Hawkins, C. J. Gallegos, M. F. Pastewait and G. L. Vaghjiani, Fourier Transform Infrared Studies in Hypergolic Ignition of Ionic Liquids, *J. Phys. Chem. A*, 2008, **112**, 7816–7824; (*f*) U. Nyberg, V. Klippmark, A. Beyglou and N. Petropoulos, Short time measurements of toxic fumes from detonation of emulsion explosive, *Swebrec Report*, 2015, **1**, ISSN 1653-5006.

18 (*a*) W. Florczuk and G. Rarata, Performance evaluation of the hypergolic green propellants based on the HTP for a future next generation spacecrafts, *53rd AIAA/SAE/ASEE Joint Propulsion Conference, AIAA Propulsion and Energy Forum*, AIAA 2017-4849, July 2017, pp. 10–12; (*b*) B. Natan, V. Perteghella and Y. Solomon, Hypergolic Ignition of Oxidizers and Fuels by Fuel Gelation and Suspension of Reactive or Catalyst Particles. *46th AIAA/ASME/SAE/ASEE Joint Propulsion Conference & Exhibit*, AIAA-papers 2010-7144, July 2010, pp. 25–28; (*c*) D. A. Castaneda and B. Natan, Experimental investigation of the hydrogen peroxide solid hydrocarbon hypergolic ignition, *Acta Astronaut.*, 2018, DOI: 10.1016/j.actaastro.2018.05.058.

19 (*a*) G. Rarata and P. Surmacz, The Safe Preparation of HTP and concentrated H_2O_2 Samples, *Transactions of the Institute of Aviation*, 2011, **217**, 121–130; (*b*) S. M. Davis and N. Yilmaz, Advances in Hypergolic Propellants: Ignition, Hydrazine, and Hydrogen Peroxide Research, *Adv. Aerosp. Eng.*, 2014, **2014**, DOI: 10.1155/2014/729313; (*c*) G. Rarata, W. Florczuk and J. Smetek, Research on Preparation and Propulsive Applications of Highly Concentrated Hydrogen Peroxide, *J. Aerosp. Sci. Technol.*, 2016, (1), 42–47; (*d*) G. Rarata and J. Smętek, Explosives based on hydrogen peroxide – A historical review and novel applications, *High-Energetic Materials*, 2016, **8**, 56–62.

20 (*a*) Y. Cong, T. Zhang, T. Li, J. Sun, X. Wang, L. Ma, D. Liang and L. Lin, Propulsive Performance of a Hypergolic H_2O_2/Kerosene Bipropellant, *J. Propul. Power*, 2004, **20**, 83–86; (*b*) J. A. Blevins, R. Gostowski and S. Chianese, An experimental investigation of hypergolic ignition delay of hydrogen peroxide with fuel mixtures, *42nd AIAA Aerospace Science meeting*, AIAA paper 2004-1335.

21 B. Natan, Y. Solomon and V. Perteghella, Hypergolic Ignition by Fuel Gelation and Suspension of Reactive or Catalyst Particles, *J. Propul. Power*, 2011, **27**, 1145–1148.

22 G. Rarata and W. Florczuk, Novel Liquid Compounds as Hypergolic Propellants with HTP, *J. KONES*, 2016, **23**, 271–278.

23 S. Schneider, T. Hawkins, Y. Ahmed, M. Rosander, L. Hudgens and J. Mills, Green Bipropellants: Hydrogen-Rich Ionic Liquids that Are Hypergolic with Hydrogen Peroxide, *Angew. Chem., Int. Ed.*, 2011, **50**, 5886–5888.

24 Y.-S. Kim, G.-H. Son, T.-K. Na and S.-H. Choi, Synthesis and Physical and Chemical Properties of Hypergolic Chemicals

such as *N*,*N*,*N*-Trimethylhydrazinium and 1-Ethyl-4-Methyl-1,2,4-Tria-zolium Salts, *Appl. Sci.*, 2015, **5**, 1547–1559.

25 (*a*) S. Schneider, T. W. Hawkins, Y. AhmedandM. Rosander, Catalytic hypergolic bipropellants, *US Pat.* 8,758,531 B1, 2014; (*b*) A. Taubert, R. Löbbicke, K. Behrens, D. Steinbrück, L. Kind, T. Zhao and C. Janiak, The ionic liquid [Bmim][$FeCl_4$] catalyzes the formation of iron doped mesoporous silica aerogels for H_2O_2 decomposition, *Matters*, 2018, DOI: 10.19185/matters.201803000004, ISSN: 2297-8240.

26 (*a*) B. Wang, L. Qin, T. Mu, Z. Xue and G. Gao, Are Ionic Liquids Chemically Stable?, *Chem. Rev.*, 2017, **117**, 7113–7131; (*b*) J. Restolho, J. L. Mata, R. Colaco and B. Saramago, Moisture Absorption in Ionic Liquid Films, *J. Phys. Chem. C*, 2013, **117**, 10454–10463.

27 (*a*) H. Xue, Y. Gao, B. Twamley and J. M. Shreeve, New Energetic Salts Based on Nitrogen-Containing Heterocycles, *Chem. Mater.*, 2005, **17**, 191–198; (*b*) H. Xue, S. W. Arritt, B. Twamley and J. M. Shreeve, Energetic Salts from N-Aminoazoles, *Inorg. Chem.*, 2004, **43**, 7972–7977; (*c*) P. D. McCrary, P. A. Beasley, O. A. Cojocaru, S. Schneider, T. W. Hawkins, J. P. L. Perez, B. W. McMahon, M. Pfeil, J. A. Boatz, S. L. Anderson, S. F. Son and R. D. Rogers, Hypergolic ionic liquids to mill, suspend, and ignite boron nanoparticles, *Chem. Commun.*, 2012, **48**, 4311–4313.

28 Q. Zhang, P. Yin, J. Zhang and J. M. Shreeve, Cyanoborohydride-Based Ionic Liquids as Green Aerospace Bipropellant Fuels, *Chem.–Eur. J.*, 2014, **20**, 6909–6914.

29 (*a*) A. Wacker, C. G. Yan, G. Kaltenpoth, A. Ginsberg, A. M. Arif, R. D. Ernst, H. Pritzkow and W. Siebert, Metal complexes of anionic 3-borane-1-alkylimidazol-2-ylidene derivatives, *J. Organomet. Chem.*, 2002, **641**, 195–202; (*b*) P. V. Ramachandran, A. S. Kulkarni, Y. Zhao and J. Mei, Amine–boranes bearing borane-incompatible functionalities: application to selective amine protection and surface functionalization, *Chem. Commun.*, 2016, **52**, 11885–11888.

30 (*a*) X. Zhang, L. Pan, L. Wang and J.-J. Zou, Review on synthesis and properties of high-energy-density liquid fuels: hydrocarbons, nanofluids and energetic ionic liquids, *Chem. Eng. Sci.*, 2018, **180**, 95–125; (*b*) V. K. Bhosale and P. S. Kulkarni, Ultrafast igniting, imidazolium based hypergolic ionic liquids with enhanced hydrophobicity, *New J. Chem.*, 2017, **41**, 1250–1258.

31 S. Huang, W. Zhang, T. Liu, K. Wang, X. Qi, J. Zhang and Q. Zhang, Towards *N*-Alkylimidazole Borane-based Hypergolic Fuels, *Chem.–Asian J.*, 2016, **11**, 3528–3533.

32 H. A. Liebhafsky, The Catalytic Decomposition of Hydrogen Peroxide by the Iodine-Iodide Couple at 25°, *J. Am. Chem. Soc.*, 1932, **54**, 1792–1806.

33 H. A. Liebhafsky and A. J. Mohammad, The Kinetics of the Reduction, in Acid Solution, of Hydrogen Peroxide by Iodide Ion, *J. Am. Chem. Soc.*, 1933, **55**, 3977–3986.

34 H. A. Liebhafsky, The Catalytic Decomposition of Hydrogen Peroxide by the Iodine–Iodide Couple. II and III. The Rate of Oxidation in Neutral, and in acid, Solution of Hydrogen Peroxide by Iodine, *J. Am. Chem. Soc.*, 1932, **54**, 3499–3508.

35 S. Furrow, Reactions of iodine intermediates in iodate-hydrogen peroxide oscillators, *J. Phys. Chem.*, 1987, **91**, 2129–2135.

36 (*a*) J.-D. Chai and M. Head-Gordon, Long-range corrected hybrid density functionals with damped atom-atom dispersion corrections, *Phys. Chem. Chem. Phys.*, 2008, **10**, 6615–6620; (*b*) J.-D. Chai and M. Head-Gordon, Systematic optimization of long-range corrected hybrid density functionals, *J. Chem. Phys.*, 2008, **128**, 084106.

37 F. Weigend and R. Ahlrichs, Balanced basis sets of split valence, triple zeta valence and quadruple zeta valence quality for H to Rn: Design and assessment of accuracy, *Phys. Chem. Chem. Phys.*, 2005, **7**, 3297–3305.

38 P. Schwerdtfeger, M. Dolg, W. H. E. Schwarz, G. A. Bowmaker and P. D. W. Boyd, Relativistic effects in gold chemistry. I. Diatomic gold compounds, *J. Chem. Phys.*, 1989, **91**, 1762–1774.